Please find the published version at:
https://www.sciencedirect.com/science/article/abs/pii/S0011916420306974

Performance of steam ejector with nonequilibrium condensation for multi-effect distillation with thermal vapour compression (MED-TVC) seawater desalination system

Chuang Wen[1], Hongbing Ding[2], Yan Yang[1, *]

[1]Faculty of Engineering, University of Nottingham, Nottingham NG7 2RD, United Kingdom

[2]Tianjin Key Laboratory of Process Measurement and Control, School of Electrical and Information Engineering, Tianjin University, Tianjin 300072, China

*Corresponding author: Yan Yang, Email: yan.yang1@nottingham.ac.uk; flyloveyang@gmail.com

Abstract: The single-phase and two-phase flow models are developed and compared for the performance evaluation of a steam ejector for the multi-effect distillation with thermal vapour compression (MED-TVC) seawater desalination system. The results show that a single-phase flow model with ignoring the phase change predicts an unphysical temperature of the steam in the supersonic flow with the minimum value of approximately 122 K, which raises the query of the formation of the ice. The two-phase wet steam model corrects the distribution of the flow parameter by predicting the heat and mass transfer during the phase change. The steam achieves the first nonequilibrium condensation process inside the primary nozzle and another four alternating condensation and re-evaporation processes. The single-phase flow model under-predicts the entropy loss coefficient by approximately 15% than the two-phase wet steam model. The performance comparison is achieved against the single-phase model to present the accuracy of the two-phase model for the steam ejector simulation. This demonstrates that the nonequilibrium condensation is essential for the performance analysis of steam ejectors for MED-TVC seawater desalination system.

Keywords: multi-effect distillation (MED); thermal vapour compression (TVC); steam ejector; seawater desalination; nonequilibrium condensation; wet steam

1. Introduction

The multi-effect distillation with thermal vapour compression (MED-TVC) seawater desalination system provides a solution for freshwater production, which achieves energy saving by upgrading the low-grade energy [1, 2]. The steam ejector, as the main part of the TVC unit, recovers the low-pressure steam from the last effect of evaporators, which accomplish high efficient utilisation of the low-grade energy [3, 4]. Thermodynamic and economic analysis has shown that the reduction of the exergy destruction in the TVC was cost-effective for the entire seawater desalination system [5]. The MED-TVC seawater desalination system also contributes to environmental protection by integrating renewable energy [6-8].

The studies on steam ejectors for MED-TVC seawater desalination system including the novel design [9], thermodynamic analysis [10] and optimisation studies [11]. Ghaebi and Abbaspour [12] integrated heat recovery steam generators to MED-TVC seawater desalination systems. The thermodynamic analysis illustrated that the novel design improved the exergy efficiency by 57.5%. Tang et al. [13] designed a new steam ejector with pressure regulation and the optimisation improved entrainment ratios by 11.77%. Tang et al. [14] also reported that the multi-optimisation of the entrainment passage can lead to an improvement of the entrainment ratio of 28.75% for the newly designed steam ejector for MED-TVC seawater desalination systems. Gu et al. [15] proposed a steam ejector with a variable geometry by inserting a spindle inside the primary nozzle and averaged entrainment ratios reached 1.39 compared to the normal ejector of 0.69. Xue et al. [16] reported a novel design of two-stage vacuum ejectors and the experimental test demonstrated that the new design provided the vacuum pressure of about 5.3 kPa compared to normal ejectors of 18.6 kPa. Sadeghi et al. [17] proposed a thermodynamic study and optimised power - ejector - desalination systems, and their study illustrated that the decrease of the total exergy destruction resulted in high temperatures at the exit of the steam ejector to produce distilled water.

Park [18] optimised steam ejectors for the seawater desalination system by introducing the swirling flow to the primary nozzle using computational fluid dynamics (CFD) modelling, which could obtain high entrainment ratios by changing the strength of the swirling flow. Sharif [19] carried out the 2D axisymmetric and three-dimensional (3D) simulation of a steam ejector and the comparison revealed that the axisymmetric simulation obtained similar results to 3D models considering the overall performance of the steam ejector. Liu et al. [20] computationally investigated the influence of area ratios on steam ejectors for MED-TVC seawater desalination systems and they found that the entrainment ratio increased from 0.025 to 0.8. Khalid et al. [21] optimised the location of steam ejectors for MED-TVC seawater desalination systems and best unit performances could be achieved by integrating the steam ejector at the middle effect regardless of the number of effects. Wang et al. [22] performed the optimising study on primary nozzles within steam ejectors for MED-TVC seawater desalination systems using CFD modelling and they showed that the overall efficiency of the steam ejector increased by 14.41%.

The aforementioned CFD and thermodynamic analysis improved the understanding of steam ejectors for MED-TVC seawater desalination systems ignoring nonequilibrium condensation processes in steam ejectors. Fortunately, the importance of the condensation phenomenon has been gradually realized in recent studies. Bonanos [23] proposed a physical model of a steam ejector with assumptions of the one-dimensional and perfect gas model without considering the condensation process, and it was emphasized that the low temperatures due to the acceleration of the fluid may lead to the condensation of the steam, thus invalidating the assumption of perfect gas behaviour. Liu et al. [24] performed a thermodynamic analysis of steam ejectors for MED-TVC seawater desalination units, which investigated the impact of condensation behaviours on steam ejectors based on the homogeneous equilibrium theory assuming that the phase change occurred instantaneously when the steam reached the saturation state. Their study reported that the condensation is a pervasive phenomenon inside steam ejectors. Tang et al. [25] carried out visualization experiments observing condensation behaviours within steam ejectors for MED-TVC seawater desalination systems. The experimental test demonstrated that massive condensing droplets were observed with nonuniform distributions of the droplet size over the cross-area plane within supersonic flows. These studies illustrate that nonequilibrium condensation processes are significant for performance evaluations of steam ejectors for MED-TVC seawater desalination systems.

The present study fills in the scientific gap including the development of the two-phase wet steam model for nonequilibrium condensation in supersonic flows, the comparison of single-phase flow and two-phase flow models for steam ejectors and the performance evaluation of a steam ejector for MED-TVC seawater desalination systems based on the two-phase flow model. Specifically, the nonequilibrium condensation process is integrated to develop a mathematical model to evaluate performances of steam ejectors for MED-TVC seawater desalination systems. The assessments of the single-phase and two-phase flow models are carried out to describe the flow features within steam ejectors. The nonequilibrium condensation processes are discussed inside steam ejectors for MED-TVC seawater desalination systems.

2. MED-TVC seawater desalination system

The MED-TVC seawater desalination system mainly consists of a seawater supply unit, multi-evaporators, a steam ejector and a condenser, as shown in Fig. 1. Seawater is fed in condensers with heat exchange between seawater and heating steam in the parallel tubes. During this pre-process in the condenser, a small quantity of the feed seawater is used as cooling water, while the main part is sprayed into each effect of the multi-evaporators, where the seawater is heated to evaporate into water vapour. The produced steam then goes into the next effect of multi-evaporators working as heating fluids inside the parallel horizontal tubes which will condense to distilled water due to the heat exchange with the feed seawater. The remaining liquid of the feed seawater is processed as brine to be drained off from the system. These processes are repeated until the last effect of multi-evaporators, where the main part of produced steam is entrained into an ejector as a recycled steam system while the other part goes into the condenser as the heating fluid to pre-heat the intake seawater.

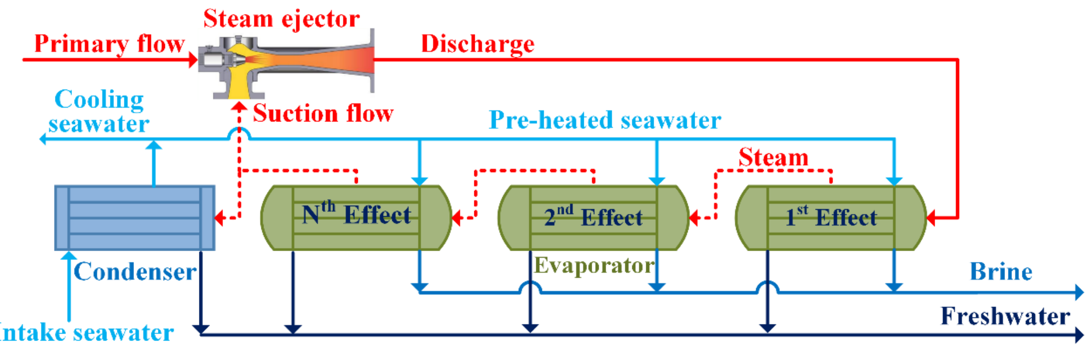

Fig. 1 Schematic diagram of a typical MED-TVC seawater desalination system

The steam ejector is an important part of MED-TVC seawater desalination systems. The motive primary flow expands in steam ejectors to entrain the low-pressure steam from the last effect of multi-evaporators. The discharge flow of steam ejectors is introduced into the first effect of the multi-evaporators as the heating fluid. This process not only saves steam consumptions for high energy efficiencies but also allows low-pressure operating conditions to eliminate the possibility of fouling and scaling. Figure 2 illustrates the schematic diagram of steam ejectors, which mainly includes five parts, namely, a primary nozzle, suction chamber, mixing section, constant section and a diffuser [26]. The dimension of the steam ejector employed for numerical simulations is described in detail in Table 1.

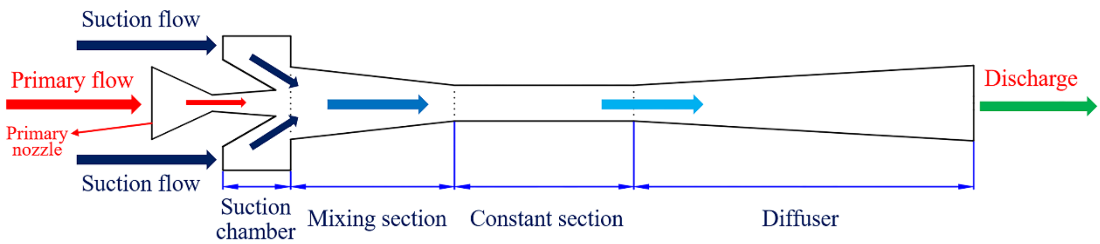

Fig. 2 Schematic diagram of a steam ejector for MED-TVC seawater desalination systems

Table 1 Dimension of the steam ejector for MED-TVC seawater desalination systems

Steam ejector dimension	Size (mm)
Inlet diameter of the primary nozzle	7.76
Throat diameter of the primary nozzle	1.76
Outlet diameter of the primary nozzle	7.00
Length of the converging part of the primary nozzle	28.70
Length of the diverging part of the primary nozzle	33.35
Inlet diameter of the mixing chamber	48.00
Length of the mixing chamber	130.00
Diameter of the constant section	19.00
Length of the constant section	95.00
Outlet diameter of the diffuser	40.00
Length of the diffuser	180.00

3. Mathematical model

Fundamental equations governing the flow features in a steam ejector are compressible Navier-Stokes equations [27-29]. Considering the complicated flow structure inside steam ejectors, including the supersonic flow, condensing flow, flow separation and shock waves, the shear stress transport (SST) *k-ω* turbulence model is employed for performance evaluations of steam ejectors for MED-TVC seawater desalination systems.

$$\frac{\partial \rho}{\partial t}+\frac{\partial (\rho u_j)}{\partial x_j}=-\Gamma \quad (1)$$

$$\frac{\partial}{\partial t}(\rho u_i)+\frac{\partial}{\partial x_j}(\rho u_j u_i)=-\frac{\partial p}{\partial x_i}+\frac{\partial \tau_{ij}}{\partial x_j}-u_i\Gamma \tag{2}$$

$$\frac{\partial}{\partial t}(\rho H)+\frac{\partial}{\partial x_j}(\rho u_j H+p)=-\frac{\partial}{\partial x_j}(\lambda_{eff}\frac{\partial T}{\partial x_j})+\frac{\partial}{\partial x_j}(u_i\tau_{ij})-h_{lv}\Gamma \tag{3}$$

$$\frac{\partial}{\partial t}(\rho k)+\frac{\partial}{\partial x_i}(\rho k u_i)=\frac{\partial}{\partial x_j}\left(\Gamma_k\frac{\partial k}{\partial x_j}\right)+\bar{G}_k-Y_k+S_k \tag{4}$$

$$\frac{\partial}{\partial t}(\rho\omega)\frac{\partial}{\partial x_j}(\rho\omega u_j)=\frac{\partial}{\partial x_j}\left(\Gamma_\omega\frac{\partial \omega}{\partial x_j}\right)+C_\omega-Y_\omega+D_\omega+S_\omega \tag{5}$$

Nonequilibrium condensation processes in steam ejectors are governed by two transport equations[30, 31]:

$$\frac{\partial(\rho Y)}{\partial t}+\frac{\partial}{\partial x_j}(\rho Y u_j)=\Gamma \tag{6}$$

$$\frac{\partial(\rho N)}{\partial t}+\frac{\partial}{\partial x_j}(\rho N u_j)=\rho J \tag{7}$$

where Γ illustrates the condensation rate of the steam:

$$\Gamma=\frac{4\pi r_c^{\ 3}}{3}\rho_l J+4\pi r^2\rho_l N\frac{dr}{dt} \tag{8}$$

$$J=\frac{q_c}{1+\phi}\frac{\rho_v^{\ 2}}{\rho_l}\sqrt{\frac{2\sigma}{\pi m_v^{\ 3}}}\exp\left(-\frac{4\pi\sigma}{3k_BT_v}r_c^{\ 2}\right) \tag{9}$$

$$\frac{dr}{dt}=\frac{\lambda_v(T_s-T_v)}{\rho_l h_{lv} r}\frac{(1-r_c/r)}{\left(\frac{1}{1+2\beta\mathrm{Kn}}+3.78(1-\nu)\frac{\mathrm{Kn}}{\mathrm{Pr}}\right)} \tag{10}$$

where J is the nucleation rate, and dr/dt is the droplet growth rate.

ANSYS FLUENT 19 [32] is utilized as a basic computational platform for conservation equations of Eqs. (1)-(5). The additional transport equations of Eqs. (6) - (7) and source terms of Eqs. (8) - (10) are integrated to ANSYS FLUENT by user-defined-scalar and user-defined-function interfaces [33]. The total pressure and total temperature boundary conditions are employed for the entrances and exit of the steam ejector [34].

4. Results and discussion

4.1. CFD validation of nonequilibrium condensations in supersonic flows

The numerical validation of nonequilibrium condensations in supersonic flows is carried out based on the case 252 of the Laval nozzle designed by Moses and Stein [35, 36], who performed the experimental measurement on the pressure distribution and the droplet size of the wet steam flow. The supersonic flow condition is assigned to the exit of the Laval nozzle. The computed pressure and droplet radius are compared against experimental data, as shown in Fig. 3. It can be observed that numerical results agree well with experimental data. Specifically, the developed CFD modelling predicts the onset of nonequilibrium condensations while calculates similar droplet radius compared to the values of experimental measurements. This demonstrates that the developed CFD modelling accurately evaluates nonequilibrium condensations in supersonic flows.

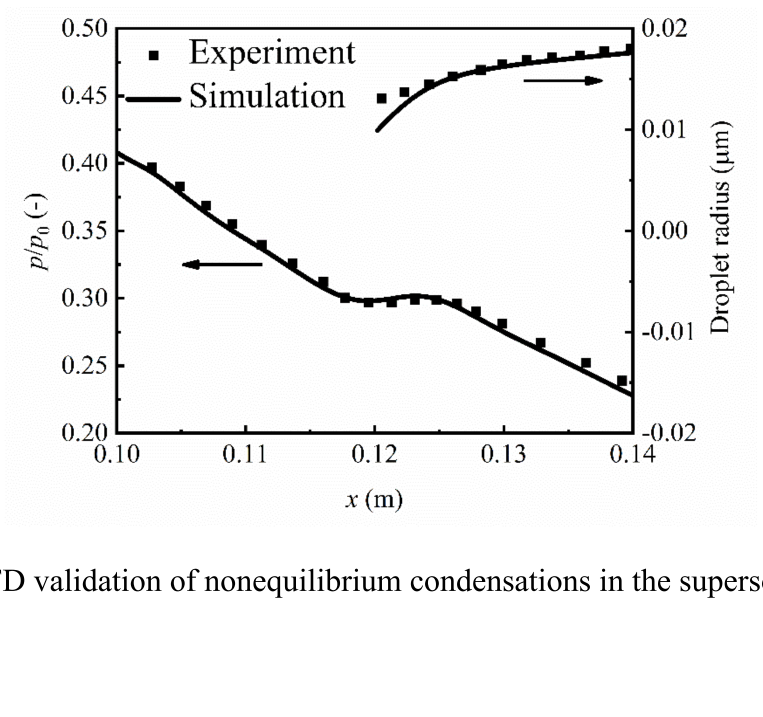

Fig. 3 CFD validation of nonequilibrium condensations in the supersonic flow

4.2. CFD validation of steam ejectors

Based on the successful validation of nonequilibrium condensations in the Moses and Stein's Laval nozzle [35, 36], the developed mathematical model is further validated for the steam ejector using experiment data reported by Sriveerakul et al. [37]. The operating conditions include the temperature of the primary flow, Tp=130 °C, the temperature of the suction flow, T_S = 5 °C, and the back pressure of discharge flow, P_b = 3000 Pa. The numerical and experimental results are described in Fig. 4. The computed pressure agrees well with experimental data in the diffuser while the numerical results are larger than experimental values in the constant section, which is attributed to the difficulty of calibrating the absolute pressure transducer near absolute zero levels [37, 38]. Thus, it is concluded that the developed nonequilibrium condensation model can be accurately used to evaluate a steam ejector for the MED-TVC seawater desalination system.

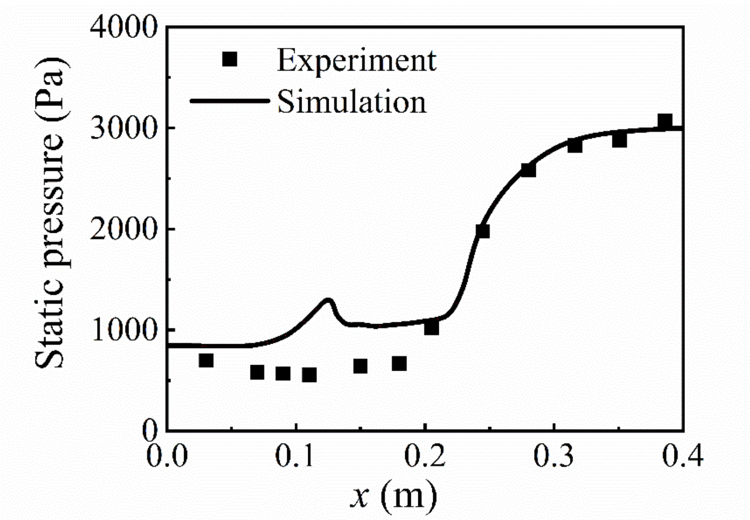

Fig. 4 CFD validation of a steam ejector for the MED-TVC seawater desalination system

4.3. Effect of single-phase and two-phase flow models

This section focuses on flow behaviours in a primary nozzle of steam ejectors for MED-TVC seawater desalination systems, which provides an opportunity to show local details on formations and developments of nonequilibrium condensation processes in supersonic flows. The quadrilateral mesh is generated for the primary nozzle, as shown in Fig. 5. Three different grids are employed for analysis of mesh independence on computational results with 16000, 42000 and 88000 cells, respectively. The flow structure is employed to show the impact of grid densities on the supersonic flow. The Mach numbers and nucleation rates in the primary nozzle are illustrated in Figs. 6 - 7. As shown in the contours & profiles of Mach numbers, the difference is observed inside the divergent part where the Mach number decreases because of heat and mass transfer of phase change processes within supersonic flows. Likewise, when looking into the detailed distribution of contours and profiles of nucleation rates, the coarse mesh calculates condensation parameters slightly different from the other two meshes. The coarse mesh predicts the peak nucleation rate of 4.52×10^{25} m^{-3} s^{-1}, while medium and fine meshes calculate the maximum value of 1.53×10^{26} m^{-3} s^{-1} and 1.94×10^{26} m^{-3} s^{-1}, respectively. Thus, the medium mesh of 42000 quadrilateral cells is utilized to carry out the computations of nonequilibrium condensations within the primary nozzle based on computational accuracies and costs.

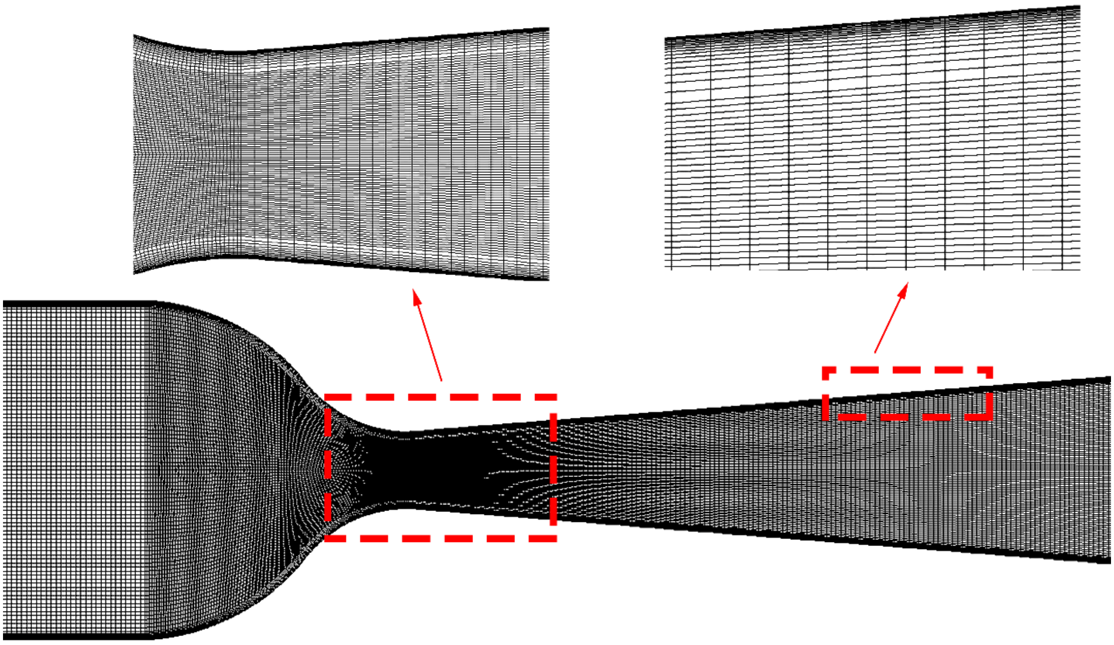

Fig. 5 Computational grid of the primary nozzle inside a steam ejector for the MED-TVC seawater desalination system

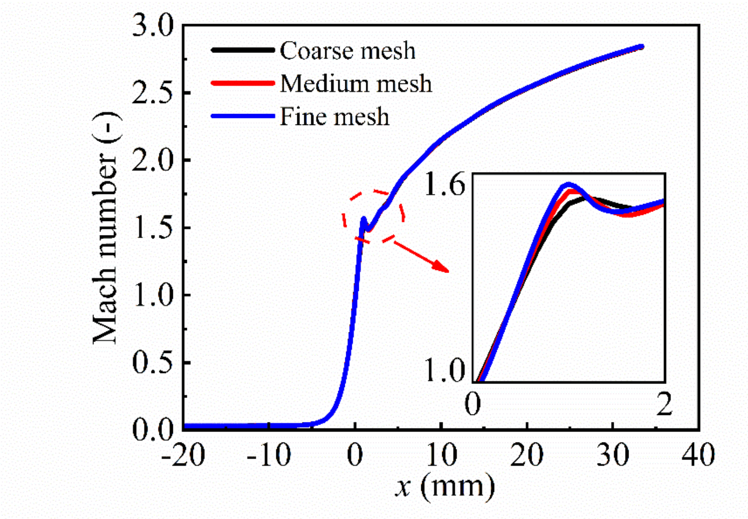

Fig. 6 Effect of grid density on the Mach number in the primary nozzle of a steam ejector

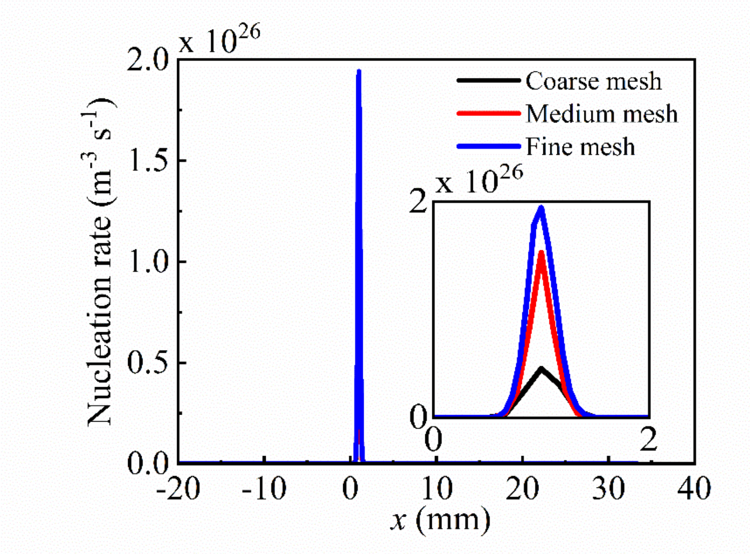

Fig. 7 Effect of grid density on the nucleation rate in the primary nozzle of a steam ejector

Steam flow reaches supersonic flows in the primary nozzle, where the rapid expansion correspondingly induces a sharp decrease of the static pressures and temperatures. The steam flow goes over the saturated-vapour line and reaches the supersaturated state inside diverging parts of primary nozzles. The extreme nonequilibrium state will lead to the occurrence of steam condensation, which is expected to influence the flow behaviour in supersonic flows. After the grid independence test, the single-phase and two-phase flow models are developed for analysing nonequilibrium condensing processes inside supersonic flows within primary nozzles.

Figures 8-10 illustrate the flow of the steam in the primary nozzle with and without considering nonequilibrium condensations, including static pressures, static temperatures and Mach numbers. It is observed that the single-phase flow represents dry steam behaviour without considering the phase change. Under the assumption of dry gas flow, the steam pressure and temperature continuously decrease within primary nozzles. For the two-phase steam flow involving the condensation process, the steam expands further to go across the saturated-vapour line, which is far from the equilibrium state to induce condensation nuclei. The latent heat release during phase changes heats the vapour phase and correspondingly results in a jump of the static pressure and static temperature. This means that the steam condensation weakens the expansion characteristics of supersonic flows within primary nozzles. For example, the Mach numbers at the nozzle exit predicted by single- and two-phase flow models reach 3.92 and 2.84, respectively. The single-phase flow model overpredicts Mach numbers by 38% compared to the two-phase flow model.

Even worse, the single-phase flow model predicts an unphysical decline of the static temperature of the steam in the supersonic flow. In this primary nozzle, the single-phase flow model predicts a static temperature of about 122 K at the nozzle exit, which may raise the query of the formation of the ice in such a low temperature. The pressure-temperature profiles of the water are shown in Fig. 11. It depicts that the pressure-temperature profile calculated by the single-phase flow model crosses the melting line and goes further to the solid region to generate the ice in such conditions. On the contrary, the pressure-temperature crosses the saturation line and stays in the liquid region due to the contribution of the phase change in supersonic flows. This demonstrates that nonequilibrium condensation processes play a significant role in performance evaluations of steam ejectors for MED-TVC seawater desalination systems.

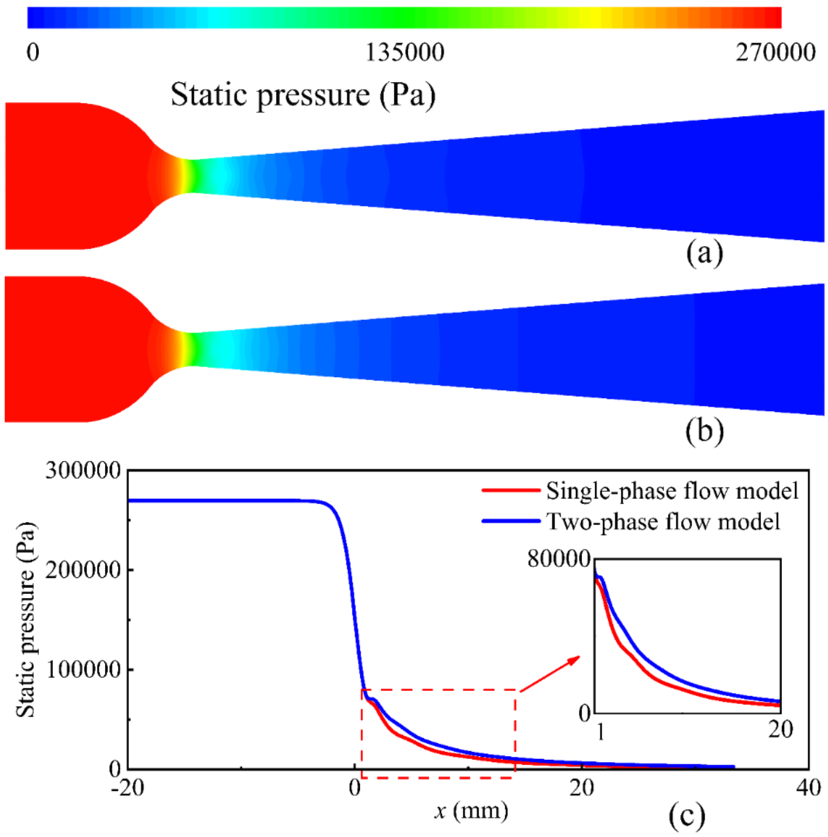

Fig. 8 Impact of condensing flow on static pressures within primary nozzles of steam ejectors: contours of single- (a) and two-phase (b) flow models, and profiles at the central axis of single- and two-phase flow models (c)

Please find the published version at:
https://www.sciencedirect.com/science/article/abs/pii/S0011916420306974

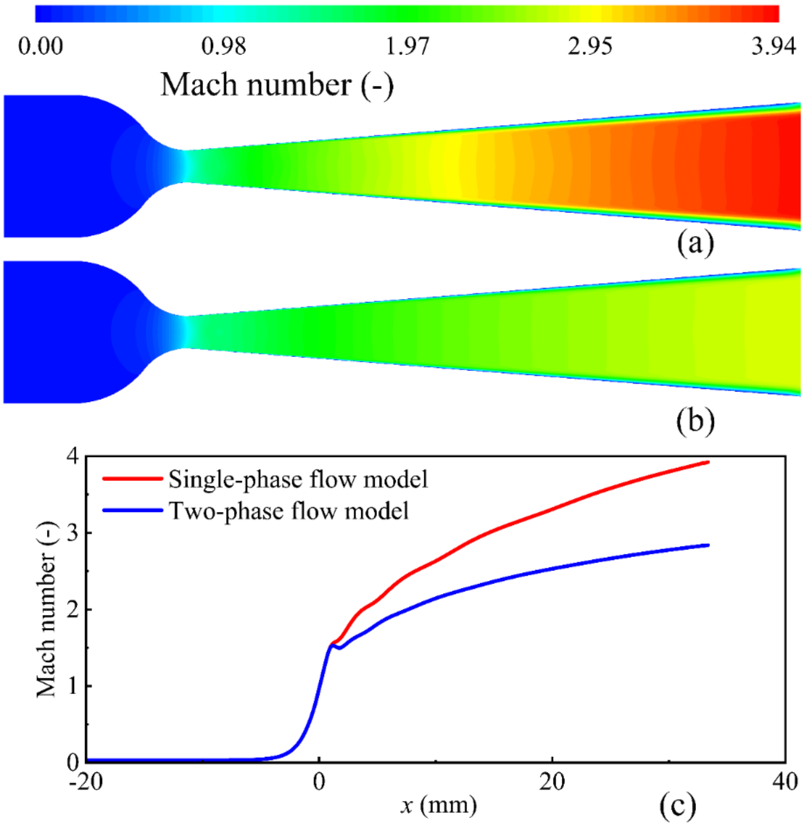

Fig. 9 Impact of condensing flow on Mach numbers within primary nozzles of steam ejectors: contours of single- (a) and two-phase (b) flow models, and profiles at the central axis of single- and two-phase flow models (c)

261 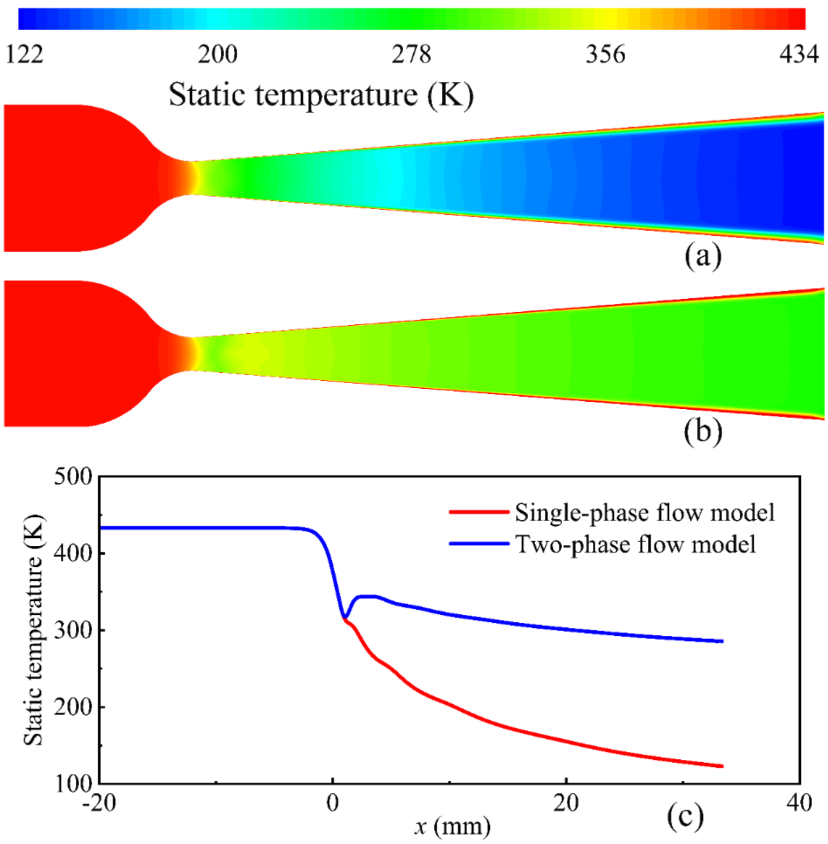

262 Fig. 10 Impact of condensing flow on static temperatures within primary nozzles of

263 steam ejectors: contours of single- (a) and two-phase (b) flow models, and profiles at

264 the central axis of single- and two-phase flow models (c)

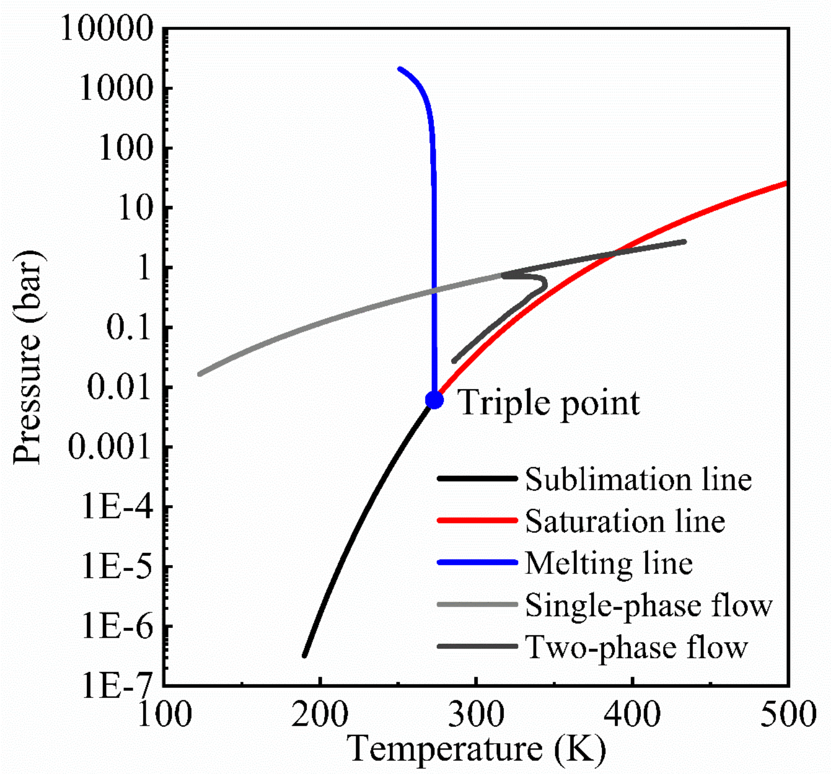

Fig. 11 Steam pressure-temperature profiles

4.4. Performance analysis of steam ejectors for MED-TVC seawater desalination systems

The quadrilateral structured mesh is generated for steam ejectors for MED-TVC seawater desalination systems, as shown in Fig. 12. The impact of gird densities on computational results of steam ejectors is carried out based on three quadrilateral structured meshes including 39000, 73000 and 168000 cells, respectively. Table 2 describes the boundary conditions of steam ejectors for MED-TVC seawater desalination systems. The high-pressure steam from the inlet of the primary nozzle is assigned to 270 kPa and 463.15 k, which will expand in the steam ejector to entrain the low-pressure steam from the suction chamber. The low-pressure steam from the last effect of the MED unit will be recirculated to the suction chamber of the steam ejector to improve the low-grade heat stream with the total pressure of 1.6 kPa and total temperature of 287.20 K. The steam with the total pressure and total temperature of 3.0kPa and 297.25 K is discharged from the exit of the ejector to the first effect of the MED unit. Fig. 13 represents the impact of mesh independence on flow behaviours in steam ejectors including static pressures, nucleation rates and entrainment ratios. It can be seen that the results based on the coarse mesh are a little bit far from the ones from medium and fine grids. Specifically, the coarse mesh predicts the maximum nucleation rate of about 4.53×10^{22} m^{-3} s^{-1}, while the medium and fine meshes compute the maximum value of 4.47×10^{26} m^{-3} s^{-1} and 4.78×10^{26} m^{-3} s^{-1}, respectively. Consequently, the medium mesh is used to evaluate the performances of steam ejectors for MED-TVC seawater desalination systems.

Table 2 Boundary condition of steam ejectors for MED-TVC seawater desalination systems

Boundary conditions	Inlet of primary nozzle	Inlet of suction chamber	Exit of steam ejector
Total pressure	270 kPa	1.6 kPa	3.0 kPa
Total temperature	463.15 K	287.20 K	297.25 K

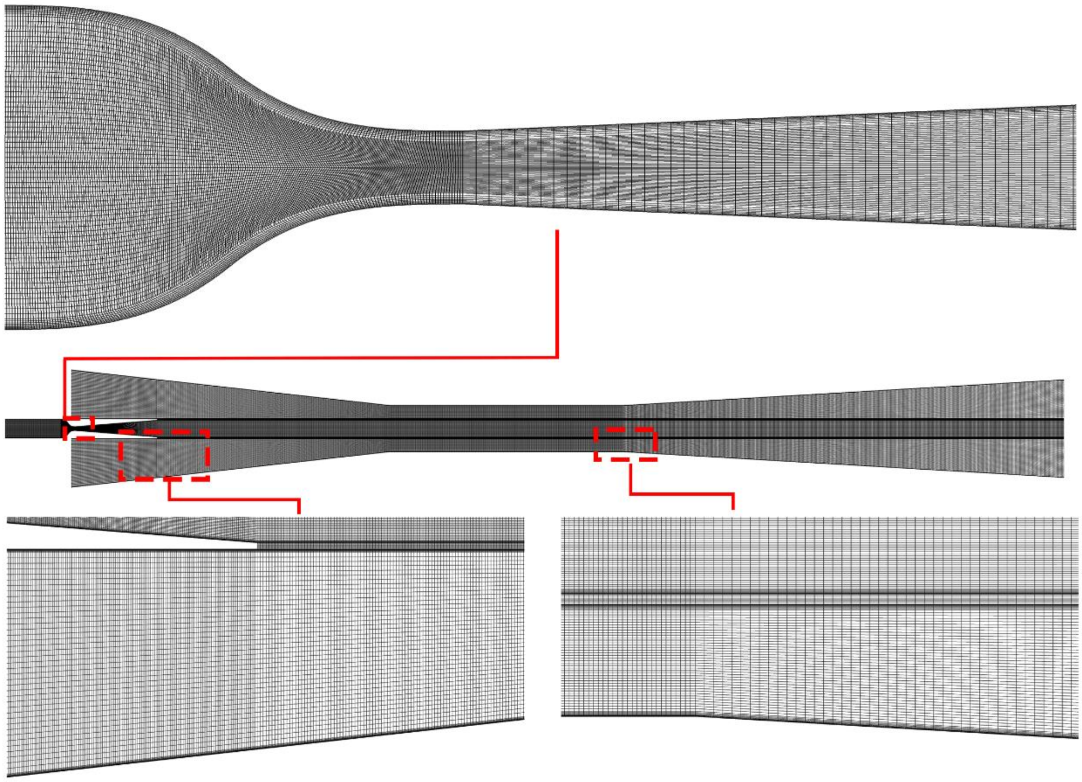

(b)

Fig. 12 Computational grids of the steam ejector for the MED-TVC seawater desalination system

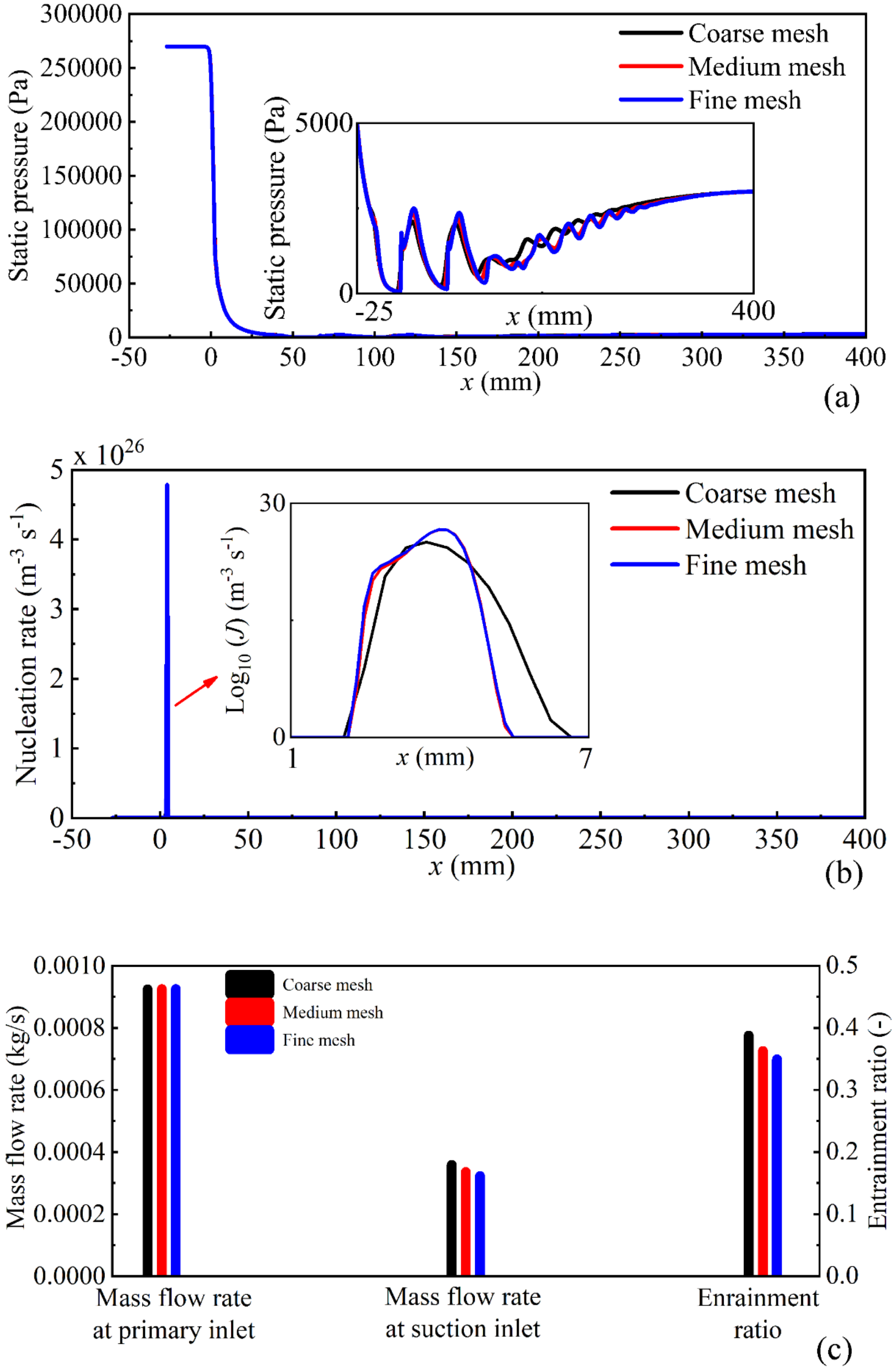

Fig. 13 Impact of the grid density on the steam ejector for the MED-TVC seawater desalination system

Figure 14 illustrates flow structures in steam ejectors for MED-TVC seawater desalination systems including Mach numbers, degrees of subcooling and nucleation rates, respectively. The steam achieves supersonic flows inside the divergent section of primary nozzles, which reaches extremely nonequilibrium state downstream the nozzle throat with a maximum degree of subcooling of about 43 K. This induces the first nucleation and condensation process of the steam with a peak nucleation rate of 4.47×10^{26} m^{-3} s^{-1}. The steam still maintains the supersonic flow downstream the condensation region, where the degree of subcooling stays at approximately 12 K till the exit plane of the primary nozzle.

The steam undergoes a further expansion-compression process to develop the under-expanded supersonic flow inside mixing and constant sections, which induces the intense change of the degree of subcooling. It can be observed that there are four expansion-compression processes of the steam in mixing and constant sections. The degree of subcooling increases to a peak value of about 38 K and then decreases sharply to the minimum value of -49 K during the first expansion-compression process, which leads to a condensation and re-evaporation process of the steam. Specifically, this further nucleation and condensation process contributes to the maximum liquid fraction of 0.19, which then declines to the trough level of 0.12 due to the re-evaporation process. This alternating condensation and re-evaporation processes occur during the four expansion-compression processes of the steam in mixing and constant sections of steam ejectors for MED-TVC seawater desalination systems.

By combining nonequilibrium condensations in the primary nozzle and four condensation and re-evaporation processes in mixing and constant sections of steam ejectors, it is observed that the peak values of degree of subcooling are gradually decreasing, while their trough levels are increasing. For instance, the first to fifth peak values of the degree of subcooling are 43 K, 38 K, 26K, 21 K, 19K, and the first to fourth trough levels are -49 K, -8 K, -6 K, -1 K, respectively. This correspondingly decreases the peak value of the nucleation rate of 4.47×10^{26} m^{-3} s^{-1}, 1.22×10^{21} m^{-3} s^{-1}, 3.85×10^{16} m^{-3} s^{-1}, 4.26×10^{10} m^{-3} s^{-1} and 1.23×10^{9} m^{-3} s^{-1} for the first to fifth condensation processes, which finally changes the first to the fourth peak value of the liquid fraction of 0.19, 0.16, 0.143, 0.141, respectively. The degree of subcooling of the steam remains above zero downstream the fourth expansion-compression flow in the constant section of steam ejectors, which makes the liquid fraction stay at around 0.14 in this region.

Please find the published version at:
https://www.sciencedirect.com/science/article/abs/pii/S0011916420306974

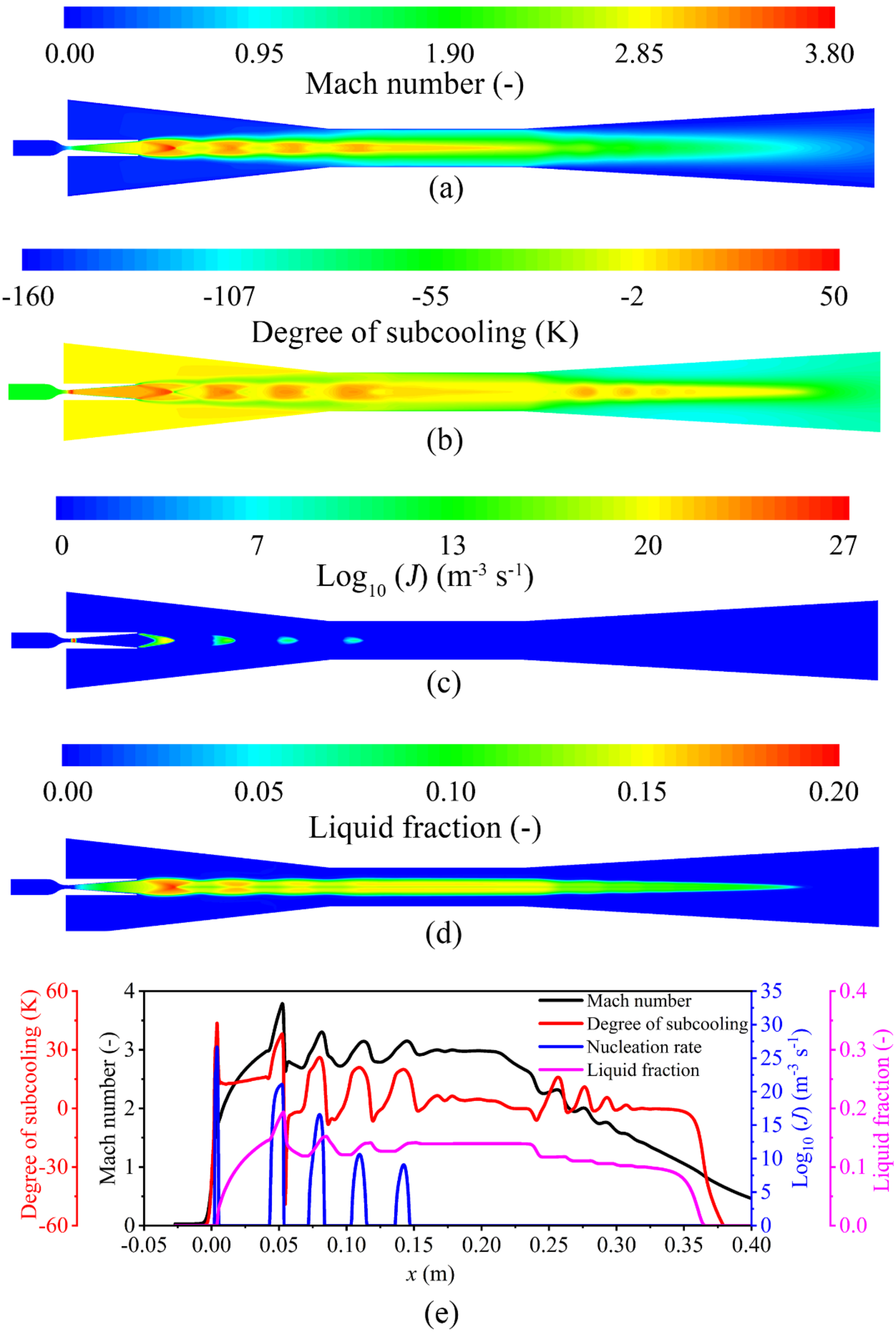

Fig. 14 Flow structures in the steam ejector for the MED-TVC seawater desalination system: contours of Mach numbers (a), contours of degrees of subcooling (b),

contours of nucleation rates (c), contours of liquid fractions (d), and profiles of Mach numbers, degrees of subcooling, nucleation rates and liquid fractions at central lines (e)

The flow structures represent the typical gas-liquid two-phase flows inside the divergent part of primary nozzles, mixing and constant sections of steam ejectors for MED-TVC seawater desalination systems, which are expected to affect energy losses within steam ejectors. The entropy loss coefficient is employed here to evaluate the loss of steam ejectors for MED-TVC seawater desalination systems. The entropy loss coefficient is a function of the enthalpy, entropy and temperature, which is defined as [39]:

$$\eta = \frac{h_{in} - h_{out}}{h_{in} - h_{out} + T_{v,out}(s_{out} - s_{in})} \tag{11}$$

where η is the entropy loss coefficient, h_{in} and h_{out} are the enthalpies at ejector inlet and outlet, s_{in} and s_{out} are the entropy at ejector inlet and outlet, $T_{v,out}$ is the steam temperature at an ejector outlet.

Table 3 describes the thermodynamic parameters and entropy loss coefficient of steam ejectors for MED-TVC seawater desalination systems based on single- and two-phase flow models, including the enthalpy, entropy and temperature of the steam at the inlet and out of steam ejectors. It can be found that the single-phase flow model ignoring phase change processes computes larger enthalpy, entropy and temperature than the two-phase flow model at ejector outlets. Subsequently, the single-phase flow model calculates the entropy loss coefficient of 0.084 while the wet steam model predicts a higher value of 0.097. That is, the dry gas model under-predicts the entropy loss coefficient by approximately 15% compared to the two-phase flow model. It demonstrates that nonequilibrium condensations play a vital role in performance analyses of steam ejectors for MED-TVC seawater desalination systems.

Table 3 Entropy loss coefficient and thermodynamic parameters of steam ejectors for MED-TVC seawater desalination systems based on single- and two-phase flow models

	h_{in} (J/kg)	s_{in} (J/(kg.K))	h_{out} (J/kg)	s_{out} (J/(kg.K))	$T_{v,out}$ (K)	η (-)	Error (%)
Dry gas	751761.15	147.59	686752.18	2056.06	368.96	0.084	15%
Wet steam	751761.65	147.59	677778.21	2031.61	364.23	0.097	-

5. Conclusions

Performance analyses of a steam ejector are carried out for MED-TVC seawater desalination systems considering nonequilibrium condensation behaviours. The single-phase flow model with ignoring phase change processes predicts an unphysical temperature of the steam in the supersonic flow with the minimum value of approximately 122 K in the primary nozzle. The two-phase flow model predicts that the steam expands further and departs from equilibrium states to induce the occurrence of the nonequilibrium condensation in supersonic flows. The flow structures in steam ejectors for MED-TVC systems illustrates that the steam reaches extremely nonequilibrium states in the steam ejector to induce the nucleation and condensation processes in the primary nozzle, mixing and constant sections. The liquid fraction stays at around 0.14 in the constant section of the steam ejector due to the nonequilibrium condensation. The single-phase flow model under-predicts the entropy loss coefficient by approximately 15% compared to a two-phase flow model. This demonstrates that nonequilibrium condensations play a crucial role in performance analyses of steam ejectors for MED-TVC seawater desalination systems

Acknowledgements

This project has received funding from the European Union's Horizon 2020 research and innovation programme under the Marie Sklodowska-Curie grant agreement No 792876 and the National Natural Science Foundation of China under Grant 51876143.

References

[1] Y. Tang, Z. Liu, Y. Li, C. Shi, Combined auxiliary entrainment and structure optimization for performance improvement of steam ejector with consideration of back pressure variation, Energy Conversion and Management, 166 (2018) 163-173.

[2] L. Guimard, A. Cipollina, B. Ortega-Delgado, G. Micale, F. Couenne, P. Bandelier, C. Jallut, New considerations for modelling a MED-TVC plant under dynamic conditions, Desalination, 452 (2019) 94-113.

[3] Y. Tang, Z. Liu, C. Shi, Y. Li, A novel steam ejector with pressure regulation to dredge the blocked entrained flow for performance improvement in MED-TVC desalination system, Energy Conversion and Management, 172 (2018) 237-247.

[4] D. Strušnik, M. Marčič, M. Golob, A. Hribernik, M. Živić, J. Avsec, Energy efficiency analysis of steam ejector and electric vacuum pump for a turbine condenser air extraction system based on supervised machine learning modelling,

Applied Energy, 173 (2016) 386-405.

[5] M.L. Elsayed, O. Mesalhy, R.H. Mohammed, L.C. Chow, Exergy and thermo-economic analysis for MED-TVC desalination systems, Desalination, 447 (2018) 29-42.

[6] A. Razmi, M. Soltani, M. Tayefeh, M. Torabi, M. Dusseault, Thermodynamic analysis of compressed air energy storage (CAES) hybridized with a multi-effect desalination (MED) system, Energy Conversion and Management, 199 (2019) 112047.

[7] B. Ghorbani, M. Miansari, S. Zendehboudi, M.-H. Hamedi, Exergetic and economic evaluation of carbon dioxide liquefaction process in a hybridized system of water desalination, power generation, and liquefied natural gas regasification, Energy Conversion and Management, 205 (2020) 112374.

[8] K. Mohammadi, M. Saghafifar, K. Ellingwood, K. Powell, Hybrid concentrated solar power (CSP)-desalination systems: A review, Desalination, 468 (2019) 114083.

[9] Y. Tang, Z. Liu, Y. Li, C. Shi, H. Wu, Performance improvement of steam ejectors under designed parameters with auxiliary entrainment and structure optimization for high energy efficiency, Energy Conversion and Management, 153 (2017) 12-21.

[10] I.B. Askari, M. Ameri, Techno economic feasibility analysis of Linear Fresnel solar field as thermal source of the MED/TVC desalination system, Desalination, 394 (2016) 1-17.

[11] C. Wang, L. Wang, X. Wang, H. Zhao, Design and numerical investigation of an adaptive nozzle exit position ejector in multi-effect distillation desalination system, Energy, 140 (2017) 673-681.

[12] H. Ghaebi, G. Abbaspour, Thermoeconomic analysis of an integrated multi-effect desalination thermal vapor compression (MED-TVC) system with a trigeneration system using triple-pressure HRSG, Heat and Mass Transfer, 54 (2018) 1337-1357.

[13] Y. Tang, Z. Liu, C. Shi, Y. Li, A novel steam ejector with pressure regulation to optimize the entrained flow passage for performance improvement in MED-TVC desalination system, Energy, 158 (2018) 305-316.

[14] Y. Tang, Z. Liu, Y. Li, C. Shi, C. Lv, A combined pressure regulation technology with multi-optimization of the entrainment passage for performance improvement of the steam ejector in MED-TVC desalination system, Energy, 175 (2019) 46-57.

[15] W. Gu, X. Wang, L. Wang, X. Yin, H. Liu, Performance investigation of an auto-tuning area ratio ejector for MED-TVC desalination system, Applied Thermal Engineering, 155 (2019) 470-479.

[16] H. Xue, L. Wang, L. Jia, C. Xie, Q. Lv, Design and investigation of a two-stage vacuum ejector for MED-TVC system, Applied Thermal Engineering, 167 (2020) 114713.

[17] M. Sadeghi, M. Yari, S.M.S. Mahmoudi, M. Jafari, Thermodynamic analysis and optimization of a novel combined power and ejector refrigeration cycle – Desalination system, Applied Energy, 208 (2017) 239-251.

[18] I.S. Park, Numerical investigation of entraining performance and operational

robustness of thermal vapor compressor having swirled motive steam inflow, Desalination, 257 (2010) 206-211.

[19] N. Sharifi, Axisymmetric and three dimensional flow modeling within thermal vapor compressors, Heat and Mass Transfer, 49 (2013) 1489-1501.

[20] J. Liu, L. Wang, L. Jia, X. Wang, The influence of the area ratio on ejector efficiencies in the MED-TVC desalination system, Desalination, 413 (2017) 168-175.

[21] K.A. Khalid, M.A. Antar, A. Khalifa, O.A. Hamed, Allocation of thermal vapor compressor in multi effect desalination systems with different feed configurations, Desalination, 426 (2018) 164-173.

[22] K. Wang, L. Wang, L. Jia, W. Cai, R. Gao, Optimization design of steam ejector primary nozzle for MED-TVC desalination system, Desalination, 471 (2019) 114070.

[23] A.M. Bonanos, Physical modeling of thermo-compressor for desalination applications, Desalination, 412 (2017) 13-19.

[24] J. Liu, L. Wang, L. Jia, H. Xue, Thermodynamic analysis of the steam ejector for desalination applications, Applied Thermal Engineering, 159 (2019) 113883.

[25] Y. Tang, Z. Liu, Y. Li, H. Wu, X. Zhang, N. Yang, Visualization experimental study of the condensing flow regime in the transonic mixing process of desalination-oriented steam ejector, Energy Conversion and Management, 197 (2019) 111849.

[26] C. Wen, B. Rogie, M.R. Kærn, E. Rothuizen, A first study of the potential of integrating an ejector in hydrogen fuelling stations for fuelling high pressure

hydrogen vehicles, Applied Energy, 260 (2020) 113958.

[27] C. Wen, N. Karvounis, J.H. Walther, H. Ding, Y. Yang, Non-equilibrium condensation of water vapour in supersonic flows with shock waves, International Journal of Heat and Mass Transfer, 149 (2020) 119109.

[28] H. Ding, Y. Li, E. Lakzian, C. Wen, C. Wang, Entropy generation and exergy destruction in condensing steam flow through turbine blade with surface roughness, Energy Conversion and Management, 196 (2019) 1089-1104.

[29] C. Wen, N. Karvounis, J.H. Walther, Y. Yan, Y. Feng, Y. Yang, An efficient approach to separate CO2 using supersonic flows for carbon capture and storage, Applied energy, 238 (2019) 311-319.

[30] A. Kantrowitz, Nucleation in very rapid vapor expansions, The Journal of chemical physics, 19 (1951) 1097-1100.

[31] J. Young, The spontaneous condensation of steam in supersonic nozzle, Physico Chemical Hydrodynamics, 3 (1982) 57-82.

[32] ANSYS Fluent Theory Guide, ANSYS Inc., USA, (2017).

[33] Y. Yang, J.H. Walther, Y. Yan, C. Wen, CFD modeling of condensation process of water vapor in supersonic flows, Applied Thermal Engineering, 115 (2017) 1357-1362.

[34] Y. Yang, X. Zhu, Y. Yan, H. Ding, C. Wen, Performance of supersonic steam ejectors considering the nonequilibrium condensation phenomenon for efficient energy utilisation, Applied Energy, 242 (2019) 157-167.

[35] C.A. Moses, G.D. Stein, On the growth of steam droplets formed in a Laval nozzle

using both static pressure and light scattering measurements, Journal of Fluids Engineering, 100 (1978) 311-322.

[36] J. Starzmann, F.R. Hughes, S. Schuster, A.J. White, J. Halama, V. Hric, M. Kolovratník, H. Lee, L. Sova, M. Šťastný, M. Grübel, M. Schatz, D.M. Vogt, Y. Patel, G. Patel, T. Turunen-Saaresti, V. Gribin, V. Tishchenko, I. Gavrilov, C. Kim, J. Baek, X. Wu, J. Yang, S. Dykas, W. Wróblewski, S. Yamamoto, Z. Feng, L. Li, Results of the International Wet Steam Modeling Project, Proceedings of the Institution of Mechanical Engineers, Part A: Journal of Power and Energy, 232 (2018) 550-570.

[37] T. Sriveerakul, S. Aphornratana, K. Chunnanond, Performance prediction of steam ejector using computational fluid dynamics: Part 1. Validation of the CFD results, International Journal of Thermal Sciences, 46 (2007) 812-822.

[38] T. Sriveerakul, S. Aphornratana, K. Chunnanond, Performance prediction of steam ejector using computational fluid dynamics: Part 2. Flow structure of a steam ejector influenced by operating pressures and geometries, International Journal of Thermal Sciences, 46 (2007) 823-833.

[39] S. Dykas, M. Majkut, K. Smołka, M. Strozik, Study of the wet steam flow in the blade tip rotor linear blade cascade, International Journal of Heat and Mass Transfer, 120 (2018) 9-17.